Optical and electrical transport properties of facing-target sputtered Al doped ZnO transparent film

Z. Q. Li[a)]
Institute of Advanced Materials Physics, Faculty of Science, Tianjin University, Tianjin 300072, People's Republic of China

D. X. Zhang
College of Information Technical Science, Nankai University, Tianjin 300071, People's Republic of China

J. J. Lin
Institute of Physics, National Chiao Tung University, Hsinchu 30010, Taiwan and Department of Electrophysics, National Chiao Tung University, Hsinchu 30010, Taiwan

(Received 29 December 2005; accepted 15 April 2006; published online 22 June 2006)

Al doped zinc oxide thin film was prepared by dc facing-target sputtering method and its structural, optical, and electrical transport properties have been investigated. The average transmittance of the films is greater than 90% in the wavelength region of 450–700 nm while the resistivity is as high as 3×10^{-3} Ω cm. The band gap energy derived from the transmission data is 3.76 eV, which is higher than that of pure ZnO thin film. This band gap growth phenomenon cannot be explained in terms of the Burstein-Moss effect. The resistivity and Hall effect measurements suggest that the interaction between the charge carriers and phonons plays a key role in the electrical transport properties of the film between 60 and 300 K. The film exhibits negative magnetoresistance at low temperatures, which can be well described by a semiempirical expression that takes into account the third order *s-d* exchange Hamiltonians describing a negative part and a two-band model for positive contribution. © *2006 American Institute of Physics*. [DOI: 10.1063/1.2204827]

I. INTRODUCTION

There has been great interest in zinc oxide semiconductor materials lately, as seen from a surge of a good number of relevant publications.[1,2] The interest in ZnO is aroused not only by the transparent conducting characteristics of doped ZnO films but also by the prospects in optoelectronic applications due to a direct wide energy gap (E_g=3.3 eV at room temperature) in this material. Doping of small amounts of IIIA elements, such as Al, Ga, and In, to ZnO results in a marked decrease in the electrical resistivity while, on the other hand, the optical transparency in the visible range of light spectrum remains high. Hence it is important to clarify the conduction mechanisms in the materials, especially in doped ZnO. The temperature dependence of the resistivity and Hall coefficient represents a key element for the understanding of the conduction mechanisms in the materials. Surprisingly, there have been few reports on the temperature behavior of these transport properties in doped ZnO in the literature.[3] In the present paper, we have prepared several Al doped ZnO films with high optical transparency by a facing-target sputtering method. Systematic electronic transport measurements, including resistivity, magnetoresistance, and Hall effect, were carried out against the temperature in wide temperature ranges.

II. EXPERIMENT

The Al doped ZnO (or ZnO:Al) thin films were deposited on glass substrate by the standard dc facing-target sputtering method. Two Al_2O_3 doped zinc oxide targets were used as the sputtering source. The weight ratio of Al_2O_3 to ZnO (both were 99.99% pure) was 5%. The base pressure of the chamber was better than 3×10^{-6} torr and the sputtering was carried out in an argon (99.999%) atmosphere of 3×10^{-2} torr. The sample holder was located at a place outside the plasma zone in our dc facing-target sputtering system. Consequently, the substrate was not directly bombarded by the plasma and thus maintained at a relative low temperature during the sputtering process. (The substrate temperature increased by about 50 K during sputtering, which was far lower than the increase occurred in the usual dc or rf sputtering systems.) Hence the dc facing-target sputtering method is a better way to deposit transparent conducting oxide films on polymer substrate. The film thickness, determined by a surface profiler (Dektak, 6 m), was 430 nm. Crystal structure and phase characterization were determined by x-ray diffraction (XRD) using Cu $K\alpha$ radiation at room temperature. The optical transmittance of the ZnO:Al film was measured in the wavelength range of 300–800 nm by using an UV-VIS-NIR (near infrared) scanning spectrophotometer (Uv-3101 PC, SHIMADZU). The resistivity was measured by a standard four-probe ac technique, and the Hall coefficient was measured by the five-contact method. The temperature dependences of the resistivity and magnetoresistance were measured using a physical property measurement

[a)]Electronic mail: zhiqingli@tju.edu.cn

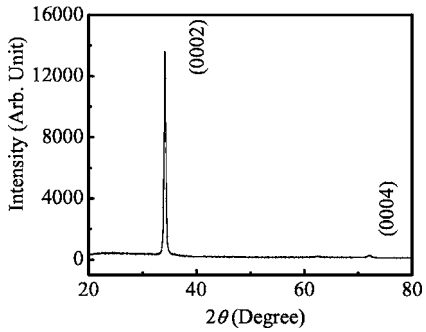

FIG. 1. X-ray diffraction pattern of the sample at room temperature.

system (PPMS-6000, Quantum Design). To confirm our data, all measurements were performed on three pieces of samples prepared at different times but under similar deposition conditions. We found that the results on all three films were identical within our uncertainties. Thus, in this report we focus our discussion on one film.

III. RESULTS AND DISCUSSION

Figure 1 shows the XRD pattern of the ZnO:Al film. In the 2θ range from 20° to 80°, we observed only two peaks located at 34.18° and 72.04°, respectively. Hence the film was single phased with a hexagonal structure characteristic to that of undoped ZnO (powder-diffraction file No. 80-0074). The two peaks at 34.18° and 72.04° correspond to the (0002) and (0004) planes, respectively, of ZnO. The XRD pattern also indicated that the c axis was the preferred orientation of the film.

Figure 2 shows the total transmission properties of the ZnO:Al film. The transmittance of the sample varies from 78.7% to 83% in the wavelength region of 400–800 nm, and the average transmittance is greater than 90% between 450 and 700 nm. This indicates the excellent optical transparency in the visible range of light spectrum for our thin film, which is of crucial importance for optoelectronic applications. Generally, the optical absorption coefficient α is defined as[4]

$$I = I_0 \exp(-\alpha d), \tag{1}$$

where I is the intensity of transmitted light, I_0 is the intensity of incident light, and d is the thickness of the thin film. Since the transmittance T_R is defined as I/I_0, we obtain α from Eq. (1),[5]

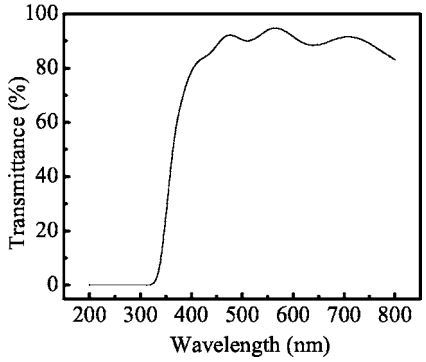

FIG. 2. Room temperature optical transmission spectra of the Al doped ZnO thin film on glass substrate.

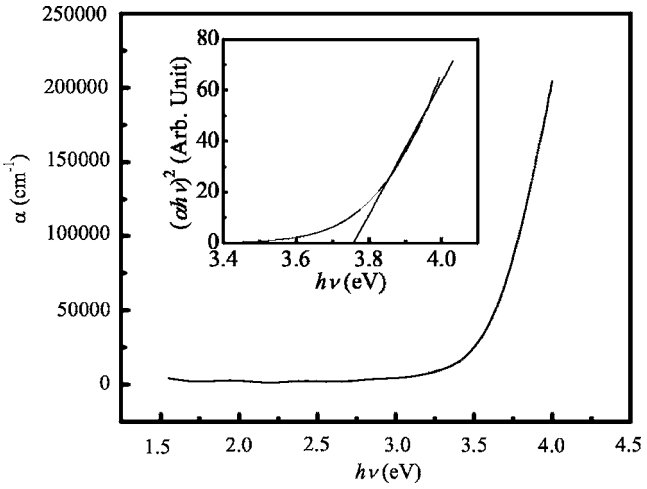

FIG. 3. Plot of absorption coefficient α with photon energy $h\nu$ for the Al doped ZnO thin film. Inset: plot of $(\alpha h\nu)^2$ against photon energy $h\nu$.

$$\alpha = -\frac{\ln T_R}{d}. \tag{2}$$

According to Tauc *et al.*,[6] for a given transition, α and photon energy $h\nu$ can be related by the expression

$$\alpha = \frac{A(h\upsilon - E_g)^{m/2}}{h\nu}, \tag{3}$$

where $m=1$ for a direct transition and $m=4$ for a indirect transition, E_g is the band gap, and A is a constant. Figure 3 plots the $(\alpha h\upsilon)^2$ against $h\nu$, from which we obtain the value of the band gap $E_g=3.76$ eV, which is higher than that of pure ZnO thin film (3.25–3.28 eV). Some other authors[7] have also observed the band gap growth phenomenon in the Al doped ZnO, but the physical origins causing such an increase are still not clarified. It is generally believed that the Burstein-Moss effect[7] plays a key role in this phenomenon: ZnO is a natural n-type material and the Fermi level would move into the conduction band when it is doped with Al. Since the states below Fermi level in the conduction band are filled, the absorption edge should shift to higher energies. If the Fermi level indeed shifts into the conduction band, the Al doped ZnO should reveal metallic characteristics as that in Sn-doped indium oxide.[8] Recently, Imai *et al.*[9] have calculated the electronic band structure of doped and undoped ZnO using density functional theory under the local density approximation. They found that the shape of the density of states curve and the band structure of doped and undoped ZnO are similar to each other, i.e., a semiconductor-to-metal transition does not occur in this system with increasing doping concentration of Al. Experimentally, Gabás *et al.*[10] have measured the valence-band spectra of pure ZnO and Al doped (1% and 3% Al concentrations) ZnO films, but they found no samples revealing any density of states around the Fermi level. Hence the Fermi level of the Al doped ZnO does not locate inside the conduction band. Physically, the band gap growth effect in the Al doped ZnO system may originate from the change in the nature and the strength of the interaction potentials between donors and the host crystals.

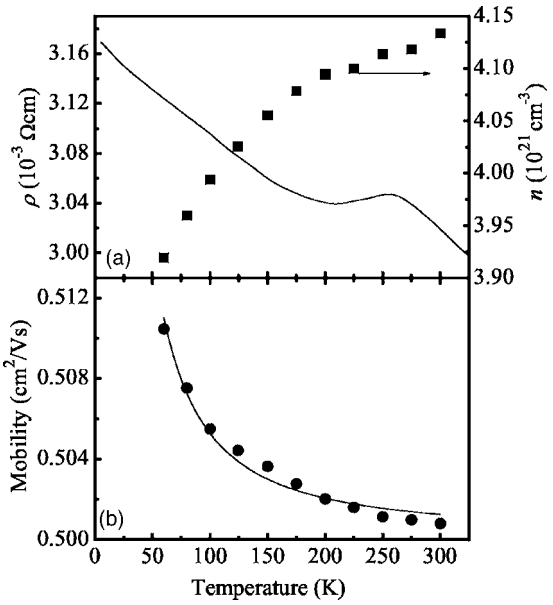

FIG. 4. (a) Resistivity (ρ) and charge carrier concentration (n) as a function of temperature; (b) temperature dependence of carrier mobility (μ) between 50 and 300 K. The solid line is the least-squares fit to Eq. (6).

Figure 4 shows a plot of the variations of the resistivity ρ, charge carrier concentration n, and carrier mobility μ with temperature for the ZnO:Al film. The charge carrier concentration is deduced from

$$R_H = -\frac{1}{ne}, \tag{4}$$

where R_H is the Hall coefficient and e is the absolute value of the electron charge. In our sample, the Hall coefficient is negative at all measuring temperatures, which confirms the n-type characteristic of the Al doped ZnO film. The carrier mobility was determined using the relation

$$\mu = \frac{1}{ne\rho}. \tag{5}$$

Generally, two scattering mechanisms should be considered in a semiconductor, i.e., scattering by phonons and by ionized impurities. At higher temperatures, the interaction between the charge carriers and phonons dominates and the temperature behavior of the carrier mobility (related to lattice scattering) can be written as[3]

$$\mu_L = A_L T^{-3/2}, \tag{6}$$

where A_L is a coefficient related to the effective mass of charge carrier. We have performed least-squares fits of our experimental data with the form $\mu = \mu_0 + \mu_L$, where μ_0 is a constant. Our best fit [the solid curve in Fig. 4(b)] is obtained with the values for the adjusting parameters $\mu_0 = 0.5003\ \mathrm{cm^2/V\,s}$ and $A_L = 4.976\ \mathrm{cm^2\,K^{3/2}/V\,s}$. The good agreement between the experiment and theory suggests that the collisions of the conduction electrons with lattice phonons are the dominant scattering process in our sample between 60 and 300 K. The temperature dependence of resistivity, shown in Fig. 4(a), does not reveal any metallic characteristic, which strongly implies that the Fermi level of the Al doped ZnO does not locate inside the conduction band. Another important feature of our sample is the small variation in the magnitude of resistivity between the wide temperature range of 2–325 K, which should benefit the device fabrication for applications.

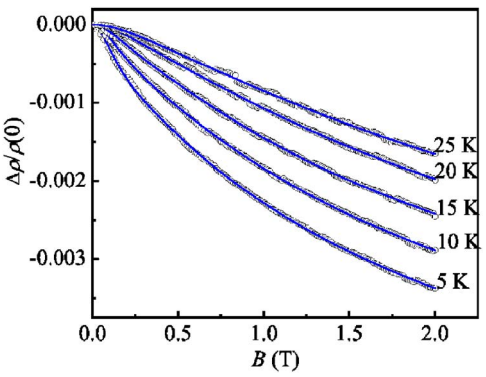

FIG. 5. (Color online) Magnetoresistance as a function of magnetic field at several temperatures as indicated. The solid lines are the least-squares fits to Eq. (7).

Figure 5 shows the magnetic field dependence of the magnetoresistance, $\Delta\rho/\rho_0$, at several temperatures between 5 and 30 K. This figure clearly indicates that the magnetoresistance is negative and its absolute value decreases with increasing temperature at a given magnetic field. Generally, two effects can lead to negative magnetoresistance in nonmagnetic materials. The first one is the weak-localization effect[11] which originates from coherent backscattering of two, time-reversed, partial electron wave amplitudes, which traverse a closed loop and returned to the origin within a timescale of τ_ϕ. The second effect originates from localized magnetic moment.[12] It has been proposed that some electrons could be localized at the donor sites giving rise to a localized magnetic moment due to statistical fluctuations in donor density and the correlation effects.[12] If the weak-localization effect plays a key role in our film, the dephasing time τ_ϕ can be extracted by fitting the low-field magnetoresistance data with three-dimensional weak-localization theoretical predictions. However, we found that the weak-localization theory[11] cannot describe our magnetoresistance data. On the other hand, our data can be fitted with the semiempirical expression proposed by Khosla and Fischer:[12]

$$\Delta\rho/\rho_0 = -a^2 \ln(1 + b^2B^2) + c^2B^2/(1 + d^2B^2). \tag{7}$$

The first term in Eq. (7) was obtained by considering the third order of the s-d exchange Hamiltonian. Here the parameters a and b are given by

$$a^2 = A_1 J \rho_F [S(S+1) + \langle M^2 \rangle] \tag{8}$$

and

$$b^2 = \left[1 + 4S^2\pi^2\left(\frac{2J\rho}{g}\right)^4\right]\frac{g^2\mu^2}{(\alpha kT)^2}, \tag{9}$$

where J is the exchange integral, ρ_F is the density of states at the Fermi energy, g is the g factor, $\langle M \rangle$ is the average magnetization, S is the spin of the localized magnetic moment, and α is a numerical constant. A_1 is regarded to be a measure of spin based scattering. The second term in Eq. (7) describes

TABLE I. Values of the parameters *a*, *b*, *c*, and *d* obtained from least-squares fits to the experimental data.

T (K)	*a*	*b*	*c*	*d*
5	0.029 43	8.015 31	0.119 45	3.110 24
10	0.029 46	5.787 99	0.097 23	2.580 46
15	0.028 79	4.351 36	0.079 08	2.247 86
20	0.029 57	2.807 01	0.053 89	1.569 17
25	0.028 92	2.225 02	0.042 19	1.326 42

a positive component of the magnetoresistance, and it can be deduced from a two-band model by solving the Boltzmann equation.[13] The parameters *c* and *d* are related to the conductivity and relaxation time of each group of carriers. The solid lines in Fig. 5 are the least-squares fits to our magnetoresistance (MR) data using Eq. (7). This figure clearly indicates that our experimental data are well described by Eq. (7), implying that the negative MR can be explained by the localized magnetic moment model when the third order of the *s-d* exchange Hamiltonian is considered. Table I lists the values of the fitting parameters at different measurement temperatures. As expected, the parameter *a* shows temperature independent characteristic and *b* is nearly linear with T^{-1}, which is consistent with the model. Since the parameters *c* and *d* are related to the magnitude of the positive MR, their decrease with increasing temperature is reasonable.[12]

IV. SUMMARY

We have measured the optical and electrical transport properties of an Al doped zinc oxide thin film fabricated by dc facing-target sputtering method. Our film shows excellent optical transparency in the visible range of light spectrum and its resistivity varies weakly with temperature over a wide temperature range of 5–330 K. We found that the band gap energy of the Al doped zinc oxide thin film is greater than that of pure ZnO thin film. This growth in band gap is ascribed to the change in the nature and strength of the interaction potentials between donors and the host crystals. The resistivity and Hall effect measurements indicate that the interaction between the charge carriers and phonons plays a key role in the electrical transport properties of the film between 60 and 300 K. We have also observed negative magnetoresistance in the sample at low temperatures and explained the behavior with a semiempirical expression which takes into account the third order *s-d* exchange Hamiltonians describing a negative part and a two-band model for the positive contribution.

ACKNOWLEDGMENTS

This work is supported by the Natural Science Foundation of Tianjin City (Contract No. 04360211) and National Natural Science Foundation of China (Nos. 10504024 and 50401002).

[1] Ü. Özgür *et al.*, J. Appl. Phys. **98**, 041301 (2005).
[2] S. J. Pearton, D. P. Norton, K. Ip, Y. W. Heo, and T. Steiner, Prog. Mater. Sci. **50**, 293 (2005).
[3] C. Calderón, G. Gordillo, and J. Olarte, Phys. Status Solidi B **242**, 1915 (2005).
[4] K. H. Kim, K. C. Park, and D. Y. Ma, J. Appl. Phys. **81**, 7764 (1997).
[5] G. K. Paul and S. K. Sen, Mater. Lett. **57**, 959 (2002).
[6] J. Tauc, R. Grigorvici, and Y. Yanca, Phys. Status Solidi **15**, 627 (1966).
[7] F. K. Shan and Y. S. Yu, J. Eur. Ceram. Soc. **24**, 1869 (2004).
[8] Z. Q. Li and J. J. Lin, J. Appl. Phys. **96**, 5918 (2004).
[9] Y. Imai, A. Watanabe, and I. Shimono, J. Mater. Sci.: Mater. Electron. **14**, 149 (2003).
[10] M. Gabás, S. Gota, J. R. Ramos-Barrado, M. Sánchez, N. T. Barrett, J. Avila, and M. Sacchi, Appl. Phys. Lett. **86**, 042104 (2005).
[11] C. Y. Wu and J. J. Lin, Phys. Rev. B **50**, 385 (1994).
[12] R. P. Khosla and J. R. Fischer, Phys. Rev. B **2**, 4084 (1970).
[13] E. H. Sondheimer and A. H. Wilson, Proc. R. Soc. London, Ser. A **190**, 435 (1947).